

NAVAL POSTGRADUATE SCHOOL

Monterey, California



THESIS

OBSERVED KINEMATICS OF WAVES IN THE SURF ZONE

by

Richard K. (Chip) Constantian Jr.

March 1999

Thesis Advisor:
Second Reader:

T.H.C. Herbers
E.B. Thornton

Approved for public release; distribution is unlimited.

1 9 9 9 0 4 1 5 0 0 5

DTIC QUALITY INSPECTED 4

REPORT DOCUMENTATION PAGE

Form Approved
OMB No. 0704-0188

Public reporting burden for this collection of information is estimated to average 1 hour per response, including the time for reviewing instruction, searching existing data sources, gathering and maintaining the data needed, and completing and reviewing the collection of information. Send comments regarding this burden estimate or any other aspect of this collection of information, including suggestions for reducing this burden, to Washington headquarters Services, Directorate for Information Operations and Reports, 1215 Jefferson Davis Highway, Suite 1204, Arlington, VA 22202-4302, and to the Office of Management and Budget, Paperwork Reduction Project (0704-0188) Washington DC 20503.

1. AGENCY USE ONLY (Leave blank)

2. REPORT DATE
March 1999

3. REPORT TYPE AND DATES COVERED
Master's Thesis

4. TITLE AND SUBTITLE
OBSERVED KINEMATICS OF WAVES IN THE SURF ZONE

5. FUNDING NUMBERS

6. AUTHOR(S)
Constantian, Richard K. (Chip) Jr.

7. PERFORMING ORGANIZATION NAME(S) AND ADDRESS(ES)
Naval Postgraduate School
Monterey, CA 93943-5000

8. PERFORMING
ORGANIZATION REPORT
NUMBER

9. SPONSORING / MONITORING AGENCY NAME(S) AND ADDRESS(ES)

10. SPONSORING /
MONITORING
AGENCY REPORT NUMBER

11. SUPPLEMENTARY NOTES

The views expressed in this thesis are those of the author and do not reflect the official policy or position of the Department of Defense or the U.S. Government.

12a. DISTRIBUTION / AVAILABILITY STATEMENT

Approved for public release; distribution is unlimited.

12b. DISTRIBUTION CODE

13. ABSTRACT (maximum 200 words)

The observed kinematics of waves in the surf zone is examined with extensive measurements from the DUCK94 experiment. Field data used in the study were obtained from vertical stacks of bi-directional current meters and a pressure sensor mounted on a rigid frame at 3 locations along a cross-shore transect in depths of 2, 4, and 8m. Observed pressure and velocity spectra are compared to transfer functions based on linear finite depth theory and a simple nonlinear model that accounts for harmonic generation in shallow water. At high frequencies, the observed vertical attenuation of horizontal velocity spectra in 8 and 4m depth is much weaker than predicted by linear theory, and generally in good agreement with the nonlinear model predictions. In 2m depth, differences between the linear and nonlinear transfer function are small and both predictions are in reasonable agreement with the observed weak vertical decay. At infragravity frequencies in shallow water depths, observed velocity spectra often show significant vertical decay that is not predicted by either model. Velocity and pressure spectra measured in 4m depth are in good agreement with the nonlinear transfer function. Pressure spectra levels at high frequencies are shown to be significantly reduced by the nonlinear Bernoulli term in the second order pressure field. Analysis of the slopes of the high-frequency tails of the observed velocity spectra shows considerable scatter with a general tendency for spectra to flatten as waves propagate through the surf zone.

14. SUBJECT TERMS

Nearshore Processes, Surf Zone, Waves

15. NUMBER OF
PAGES
54

16. PRICE CODE

17. SECURITY CLASSIFICATION OF
REPORT
Unclassified

18. SECURITY CLASSIFICATION OF
THIS PAGE
Unclassified

19. SECURITY CLASSIFI- CATION
OF ABSTRACT
Unclassified

20. LIMITATION
OF ABSTRACT
UL

Approved for public release; distribution is unlimited.

OBSERVED KINEMATICS OF WAVES IN THE SURF ZONE

Richard K. (Chip) Constantian Jr.
Lieutenant, United States Navy
B.S. University of South Carolina

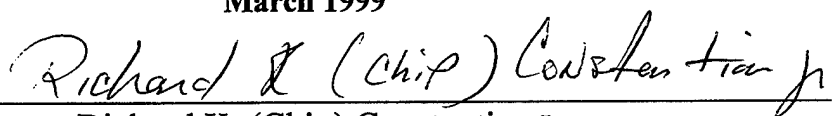
Submitted in partial fulfillment
of the requirements for the degree of

MASTER OF SCIENCE IN PHYSICAL OCEANOGRAPHY


from the

NAVAL POSTGRADUATE SCHOOL
March 1999

Author:


Richard K. (Chip) Constantian Jr.

Approved by:


T.H.C. Herbers, Thesis Advisor



E.B. Thornton, Second Reader



R.W. Garwood, Chairman
Department of Oceanography

ABSTRACT

The observed kinematics of waves in the surf zone is examined with extensive measurements from the DUCK94 experiment. Field data used in the study were obtained from vertical stacks of bi-directional current meters and a pressure sensor mounted on a rigid frame at 3 locations along a cross-shore transect in depths of 2, 4, and 8m. Observed pressure and velocity spectra are compared to transfer functions based on linear finite depth theory and a simple nonlinear model that accounts for harmonic generation in shallow water. At high frequencies, the observed vertical attenuation of horizontal velocity spectra in 8 and 4m depth is much weaker than predicted by linear theory, and generally in good agreement with the nonlinear model predictions. In 2m depth, differences between the linear and nonlinear transfer function are small and both predictions are in reasonable agreement with the observed weak vertical decay. At infragravity frequencies in shallow water depths, observed velocity spectra often show significant vertical decay that is not predicted by either model. Velocity and pressure spectra measured in 4m depth are in good agreement with the nonlinear transfer function. Pressure spectra levels at high frequencies are shown to be significantly reduced by the nonlinear Bernoulli term in the second order pressure field. Analysis of the slopes of the high-frequency tails of the observed velocity spectra shows considerable scatter with a general tendency for spectra to flatten as waves propagate through the surf zone.

TABLE OF CONTENTS

I.	INTRODUCTION	1
II.	FIELD EXPERIMENT AND DATA ANALYSIS	7
III.	VERTICAL ATTENUATION OF WAVE ORBITAL VELOCITIES	9
IV.	NONLINEAR EFFECTS ON THE PRESSURE-VELOCITY TRANSFER FUNCTION.....	15
V.	SIMILARITY OF VELOCITY SPECTRA AT HIGH FREQUENCIES	19
VI.	SUMMARY	23
	APPENDIX	27
	LIST OF REFERENCES.....	41
	INITIAL DISTRIBUTION LIST.....	43

ACKNOWLEDGMENTS

I would like to gratefully acknowledge the guidance, support, and patience of my advisor, Thomas Herbers. This paper would have never evolved without him. I would also like to thank Paul Jessen for his magic at turning ideas into code. Sincere appreciation is extended to my parents who somehow knew all the right things to say during the difficult moments and to my soon to be wife (6 days as of this writing), Jenifer, whose encouragement, love and support were instrumental in the accomplishment of this awesome endeavor.

I. INTRODUCTION

Ocean surface gravity waves (frequencies nominally between 0.05 and 0.5 Hz) are the primary driving force for nearshore currents and sediment transport. As waves propagate across the beach, their characteristics change dramatically owing to linear (e.g. shoaling and refraction) and nonlinear (e.g. wave-wave interactions and breaking) processes. Whereas the nonlinear dynamics of wave evolution across the beach has been investigated in detail, the kinematics of the associated orbital motion and its variation over the water column has received less attention. In the present study local wave properties in the surf zone are examined with velocity and pressure data collected on a natural beach (Elgar et al., 1997).

Linear theory is often used to predict wave-induced subsurface particle velocities and pressure variations. In the linear approximation, the wave field is composed of a linear superposition of sinusoidal wave components with frequency f and wavenumber k that obey the dispersion relation (Figure 1b)

$$f = \frac{1}{2\pi} [gk \tanh(kh)]^{1/2} \quad (1)$$

The associated wave induced velocity ($E_u(f; z)$, $E_v(f; z)$, $E_w(f; z)$) and pressure ($E_p(f; z)$) spectra measured at an arbitrary vertical elevation z are given by the simple linear transfer functions

$$E_u(f; z) + E_v(f; z) = \left(\frac{gk}{2\pi f} \right)^2 E_\eta(f) \frac{\cosh^2 kd}{\cosh^2 kh} \quad (2a)$$

$$E_w(f; z) = \left(\frac{gk}{2\pi f} \right)^2 E_\eta(f) \frac{\sinh^2 kd}{\cosh^2 kh} \quad (2b)$$

$$E_p(f; z) = E_\eta(f) \frac{\cosh^2 kd}{\cosh^2 kh} \quad (2c)$$

where h is the total water depth, $d (=z+h)$ is the height of the measurements above the seafloor (Figure 2), u, v are the horizontal (x, y) velocity components, w is the vertical (z) velocity component, p is pressure (divided by ρg to yield equivalent hydrostatic surface or pressure head displacements), and $E_\eta(f)$ is the spectrum of the sea surface elevation function $\eta(x, y, t)$. Equations (2a-c) are widely used to infer surface elevation spectra from subsurface pressure or velocity measurements.

The linear dispersion relation (1) and spectral transfer functions (2a-c) have been tested with extensive measurements in a range of water depths. Thornton and Krapohl (1974) measured surface height variations and orbital velocities at different vertical elevations in relatively deep (19m) water and compared the measured spectral transfer functions with the linear transfer functions (2a-c). Results show that the measurements of

horizontal and vertical velocity components in the upper part of the water column were in good agreement with linear theory over a wide frequency band (0.04-0.35 Hz) (errors less than 4-6%). Herbers and Guza (1991, 1992 and 1994) and Herbers et al. (1992) examined the dispersion relation and pressure-velocity transfer functions with measurements collected in shallower depths (7 and 13m). Results of these studies show excellent agreement at the dominant wave frequencies (errors less than 2%) with linear theory.

Whereas the linear dispersion relation (1) and transfer functions (2a-c) are generally accurate near the spectral peak frequency, significant discrepancies are typically observed at higher frequencies where energy levels are relatively low. These deviations are caused primarily by nonlinear interactions in which a pair of spectral components with frequencies f_1 and f_2 excites a bound secondary wave with the sum frequency $f_1 + f_2$ that does not obey the linear dispersion relation (Eq. 1) (e.g. Donelan et al., 1985; Herbers and Guza, 1991, 1992, 1994; Herbers et al., 1992, 1994). In shallow water depths ($kh \ll 1$), these so-called triad interactions are near-resonant, and the nonlinear energy transfers to higher frequencies are strongly enhanced (e.g. Freilich and Guza, 1984; and many others). Assuming for simplicity a narrow spectrum of waves with a peak frequency f_p , that are refracted to near normal incidence, energy is transferred primarily from the spectral peak components with $f \approx f_p$ and $k \approx k_p$ (given by (1)) through multiple triad interactions to harmonic components with frequencies and wavenumbers $(2f_p, 2k_p)$, $(3f_p, 3k_p)$, If the spectral peak components are in shallow

water ($k_p h \ll 1$) then the peak frequency (f_p) and wavenumber (k_p) obey the shallow water dispersion relation (the small kh limit of (1)):

$$f = \frac{(gh)^{1/2}}{2\pi} k \quad (3)$$

It follows that the harmonic components ($2f_p, 2k_p$), ($3f_p, 3k_p$), ... also obey (3) yielding an almost nondispersive wave field in which all wave components propagate with the shallow water wave speed $(gh)^{1/2}$. In this simple nonlinear model, high frequency components of the spectrum have wavenumbers (Eq. 2) that are smaller than those predicted by the linear dispersion relation (1). The implications of these deviations from the linear dispersion relation are illustrated in Figure 1a with a typical measured velocity spectrum in 4m depth. The measured spectrum is narrow with $f_p \approx 0.08$ Hz, with distinct harmonic peaks at $2f_p$, $3f_p$, $4f_p$ and $5f_p$. The predicted shallow water wavenumbers of the higher harmonic components are significantly smaller (16% at $3f_p$, 27% at $4f_p$, 35% at $5f_p$) than those predicted for linear waves with the same frequencies (Figure 1b).

Few measurements of wave kinematics in the surf zone have been reported. Guza and Thornton (1980) compared pressure, sea surface elevation and velocity spectra measured outside and inside the surf zone with the linear transfer functions (2). The

results indicated reasonably good agreement (errors $O(20\%)$). Vertical variation of wave properties over the water column were not sampled in this experiment.

In the present study, velocity and pressure spectra measured inside and outside the surf zone are compared with linear (2) and nonlinear transfer functions. Field data used in this study were obtained from vertical stacks of current meters with a co-located pressure sensor in depths of 2, 4, and 8m. The field data and analysis are described in Chapter II. The vertical attenuation of wave orbital velocities is investigated in Chapter III. Nonlinear effects on the pressure-velocity transfer function are examined in Chapter IV. Observed slopes of the high-frequency tail of velocity spectra in the surf zone are discussed in Chapter V, followed by a summary in Chapter VI.

II. FIELD EXPERIMENT AND DATA ANALYSIS

Detailed measurements of the shoaling evolution of waves across the inner continental shelf and beach were collected during the DUCK94 experiment at the U.S. Army Corps of Engineers Field Research Facility located near Duck, North Carolina on a straight barrier island exposed to the Atlantic Ocean. Three rigid frames (in 2, 4, and 8m water depth) were deployed along an 885 meter-long cross-shore transect (Figure 3). Each of these towers supported a stack of Marsh-McBirney electromagnetic current meters (Elgar et al., 1997, Lentz et al., 1999) and a Setra pressure sensor. Data were collected nearly continuously during September and October, 1994, with a sample frequency of 2 Hz. The 8m frame failed on October 10, during a severe storm.

The two-month observation period spans a wide range of conditions including two major nor'easter events with maximum significant wave heights of 2.5 and 3.8m and wide surf zones extending across the entire instrumented transect. Shoaling of nonbreaking waves was observed during many calm periods with significant wave heights as small as 0.2m. The observations include narrow spectra of remotely generated swell, broad spectra of locally generated seas, and bimodal spectra of mixed swell-sea systems (Elgar et al., 1997). The beach profile during the experiment featured a well developed sand bar approximately 100m from shore (Figure 3). Seaward of the sand bar, the bottom profile was nearly planar with a gentle ($\approx 1:200$) slope. Intense wave breaking often occurred on the shallow ($h \approx 1.5\text{-}2.0$ m at low tide) crest of the sand bar.

The 2m frame is located in a trough between the bar crest and a steep ($\approx 1:20$) beach face. Changes in the bathymetry were small in the first 1.5 months of the experiment, but during the most severe storm in the middle of October the sand bar moved about 80m offshore (Gallagher et al., 1998).

The present study is focused on wave kinematics in the strongly nonlinear regimes of breaking or nearly breaking waves. Therefore the analysis was limited to 125 one-hour-long data records collected at low tide with incident significant wave heights $H_s > 1.25\text{m}$, when significant wave breaking occurred on the crest of the sand bar (Herbers et al., 1999). Spectra of the horizontal velocity components ($E_u(f; z)$, $E_v(f; z)$) and pressure ($E_p(f; z)$) with a frequency bandwidth of 0.0078 Hz (56 degrees of freedom) were estimated from detided data records. Accurate estimates of the height d of instruments above the seafloor were available from continuous sonar altimeter measurements collected on each frame (Gallagher et al., 1998). The gain accuracies of the bidirectional current meters and pressure sensors are estimated to be $\pm 5\%$ and $\pm 1\%$, respectively (Guza et al., 1988).

III. VERTICAL ATTENUATION OF WAVE ORBITAL VELOCITIES

The vertical attenuation of velocity spectra observed in 2, 4, and 8m depth is examined in Figures 4-7 for four data runs that span a wide range of wave conditions, including two major nor'easters that passed through the region (Cases I and IV), energetic swell (Case II), and a local wind sea (Case III). The total horizontal velocity spectrum $E_u(f) + E_v(f)$ observed at different vertical elevations shows the expected strong attenuation at high frequencies (Figures 4-7, panels a-c). For each stack, the observed attenuation of velocity spectra between the uppermost and lowermost current meters is compared to the theoretical transfer function (2a) using two different approximations for the wavenumber k (Figures 4-7, panels d-f). The first of these approximations uses the linear finite depth dispersion relation (1) valid for free linear waves in any depth. In the second approximation, the shallow water dispersion relation (3) is used to describe the attenuation of a nonlinear wave field in shallow water that is dominated at high frequencies by nonlinearly forced harmonics (e.g., Figure 1b).

A. CASE I: SEPTEMBER 4

Energetic wind seas (H_s in 8m depth is 1.92m) were observed on September 4 during the first nor'easter (Figure 4). In 8m depth the velocity spectra are relatively broad with a peak frequency $f_p = 0.10$ Hz (Figure 4c). Root mean square velocities measured at the uppermost current meters decrease from 80 cm/s in 8m depth to 78 cm/s in 4m depth

to 45 cm/s in 2m depth. Both the 4 and 2m stacks were inside the surf zone. Nonlinear energy transfers from the incident wind wave frequencies to both higher and lower frequencies are evident in the observed evolution of spectra from 8 to 2m depth. Sum interactions cause a broadening of the spectrum and produce a weak second harmonic ($2f_p$) peak in 4m depth that appears to be dissipated in 2m depth. Spectral levels at infragravity frequencies (< 0.04 Hz) are strongly amplified as the depth decreases, and in 2m depth the spectral peak has shifted from the incident (0.1 Hz) sea peak to an infragravity (0.015 Hz) peak.

In 8m depth (Figure 4c), the attenuation of the velocity spectrum between the uppermost and lowermost current meters increases strongly with increasing frequency, from about 20% at f_p to a factor of 10 at 0.35 Hz. The analysis of 8m stack data was restricted to the range of 0-0.35 Hz because the signal levels at higher frequencies were sometimes below the noise floor for the lower current meters. The linear finite depth model overpredicts the attenuation at frequencies above f_p (Figure 4f). The errors increase with increasing frequency from only 2% at f_p to a factor of 10 at 0.35 Hz. The nonlinear model is generally in closer agreement with the observations but underpredicts the attenuation (maximum error 30% at 0.35 Hz). These comparisons show the importance of nonlinearity at high frequencies, but the nonlinear model used here is obviously inaccurate at this relatively deep site.

The observed attenuation of velocity spectra in 4m depth between the uppermost and lowermost current meters increases from 10% at f_p to 65% at 0.5 Hz. Similar to the

8m comparisons, the linear model overpredicts the attenuation in 4m depth with errors increasing from 2% at f_p to a factor of 15 at 0.5 Hz. The nonlinear model prediction is in excellent agreement with the observed attenuation at high frequencies. In 2m depth (Figure 4a) the observed attenuation is weak (< 40% at 0.5 Hz) and in reasonable agreement (typical errors of $O(10\%)$) with both the linear and nonlinear model predictions. In all three depths the observed attenuation at infragravity frequencies is significant (15-30%) whereas both models predict negligible attenuation for these long wavelength waves. These discrepancies suggest that bottom boundary layer effects may be important (i.e. vertical shear) or other motions than long gravity waves contribute to infragravity velocities (e.g., instabilities of the longshore current).

B. CASE II: SEPTEMBER 4

This data set collected one day after Case I, when the storm had moved offshore, features a narrower swell spectrum with a peak frequency $f_p=0.09$ Hz (Figure 5). The offshore significant wave height is reduced to 1.5m, and rms velocities measured with the uppermost current meters initially increase from 56 cm/s in 8m depth to 69 cm/s in 4m depth followed by a decrease to 46 cm/s in 2m depth. As the waves shoal from 8 to 4m depth, large nonlinear energy transfers in sum interactions produced clearly distinguishable harmonic peaks at $2f_p$, $3f_p$, and $4f_p$ (Figure 5b). In 2m depth (Figure 5a), these harmonic peaks are obliterated by intermittent wave breaking on the sand bar (Figure 3). As in Case I, infragravity velocity spectral levels are strongly enhanced during

shoaling and dominate the spectra observed at the 2m stack (Figure 5a). The vertical attenuation of velocity spectra is similar to Case I. In 8 and 4m depth, the observed attenuation is much weaker than predicted by linear theory and in good agreement with the nonlinear prediction (errors less than 30% and 10% in 8 and 4m depth, respectively). In 2m depth the observed decay is weak and in good agreement with both model predictions (except for a stronger observed decay at infragravity frequencies).

C. CASE III: SEPTEMBER 19

The third case is characterized by less energetic (offshore $H_s = 0.82\text{m}$) high frequency ($f_p = 0.17\text{ Hz}$) seas. The rms horizontal velocities measured with the uppermost current meters are 45, 58 and 47cm/s at the 2, 4, and 8m stack, respectively. These small variations suggest that wave breaking and associated energy losses occurred primarily shoreward of the 2m stack. The spectra are featureless in 8 and 4m depth but show a pronounced second harmonic peak in 2m depth ($2f_p \approx 0.3\text{ Hz}$) that is almost as large as the primary ($f_p \approx 0.15\text{ Hz}$) peak (Figure 6a). At all three stacks the observed vertical attenuation of velocity spectra is stronger than in Cases I and II (Figure 6, panels a-c). At the highest frequencies considered the observed attenuation varies between a factor 2 in 2m depth to a factor 30 in 8m depth. The observed spectral attenuation is generally in good agreement with the linear finite depth transfer function, except at very high frequencies in 8 and 4m depth where the observed attenuation falls between the stronger decay predicted by the linear transfer function and the weaker decay predicted

by the nonlinear transfer function (Figure 6, panels b,c). These comparisons suggest that the high frequency tail of the spectrum contains a mix of free waves that obey the linear dispersion relation and longer wavelength forced waves.

D. CASE IV: OCTOBER 15

The final case is from the second major nor'easter when the offshore significant wave height reached a maximum ($H_s \approx 3.8\text{m}$). No data was available from the 8m stack which had collapsed earlier during this storm. The rms velocities measured by the uppermost current meters in the 4 and 2m stacks were 76 and 53 cm/s, respectively. The spectra show strong nonlinear evolution between the 4 and 2m stacks similar to Case I. In 2m depth, the incident wave spectral peak ($f_p = 0.1\text{ Hz}$) is accompanied by distinct second and third harmonic peaks ($2f_p, 3f_p$) and a prominent infragravity peak ($f = 0.02\text{ Hz}$) (Figure 7a). Similar to cases I and II the observed vertical spectral attenuation is weak (from less than 10% at f_p to less than a factor of 2 at 0.5 Hz) (Figure 7, panels a,b), and in good agreement with the nonlinear model prediction (errors less than 30%) (Figure 7 c,d).

The case studies generally support the hypothesis that the high frequency tail of velocity spectra in shallow water is dominated by nonlinearly forced waves that propagate with the shallow water wave speed $(gh)^{1/2}$ and have a much weaker vertical decay than predicted by linear wave theory. The weak vertical attenuation of the

nonlinearly forced high-frequency wave motion is examined in Figure 8 for all 125-one-hour-long data records. The observed attenuation of the velocity variance in the high-frequency range of 0.3-0.5 Hz between the uppermost and lowermost current meter of each stack is compared to predictions based on linear (Eq. 2a with k given by Eq. 1) and nonlinear (Eq. 2a with k given by Eq. 3) transfer functions. No results for the 8m stack are presented because few data records were available and the relatively weak high frequency spectral levels were often below the instrument noise floor. In 4m depth, nonlinear model predictions (Eqs. 2a, 3) of the attenuation are in good agreement with observations (errors less than 30%) whereas the linear model consistently overpredicts the attenuation (errors between 30% and a factor 5). In 2m depth, both model predictions are in good agreement with the observations (errors less than 30%).

IV. NONLINEAR EFFECTS ON THE PRESSURE-VELOCITY TRANSFER FUNCTION

The analysis of velocity spectra in shallow water presented in Chapter III shows that the linear finite depth dispersion relation is inaccurate at high frequencies because the high-frequency tail of the spectrum is usually dominated by nonlinearly forced waves that propagate with the speed of the spectral peak components. Additional errors in the pressure-velocity transfer functions (2a-c) are introduced by the neglected nonlinear Bernoulli term in the second-order pressure field. The nonlinear pressure-velocity transfer function is examined here with a simple model for uni-directional waves in shallow water.

Assuming irrotational flow and unidirectional waves propagating in the x -direction, the horizontal orbital velocity u and pressure p can be expressed in terms of a velocity potential function $\Phi(x, z, t)$

$$u = \frac{\partial \Phi}{\partial x} \quad (4)$$

$$p = -\frac{1}{g} \left(\frac{\partial \Phi}{\partial t} + \frac{1}{2} \left(\frac{\partial \Phi}{\partial x} \right)^2 \right) \quad (5)$$

Based on the observations presented in Chapter III, we assume that the local velocity potential can be described approximately by a spectrum of wave components that all

propagate with the shallow water wave speed $(gh)^{1/2}$. The velocity potential function Φ is expressed as a general Fourier integral of the form

$$\Phi(x, z, t) = \int_{-\infty}^{\infty} \exp(i(kx - 2\pi ft)) \frac{\cosh(k(z+h))}{\cosh kh} dA(f) \quad (6)$$

with $dA(f)$ the Fourier amplitude at the surface of waves with frequency f , and the wavenumber k given by the shallow water dispersion relation (3).

Substituting (6) in (4) and (5) and evaluating the velocity $(E_u(f; z))$ and pressure $(E_p(f; z))$ spectra yields the following nonlinear transfer function (Herbers et al., 1999):

$$E_p(f; z) = \frac{h}{g} E_u(f; z) + \varepsilon_b \quad (7)$$

where ε_b is the nonlinear Bernoulli correction term that can be expressed in terms of the velocity bispectrum $B_u(f_1, f_2; z)$ (e.g., Elgar and Guza, 1985)

$$\varepsilon_b = -h^{\frac{1}{2}} g^{\frac{-3}{2}} \operatorname{Re} \left\{ \int_0^f B_u(f', f-f') df' + 2 \int_0^\infty B_u(f', f) df' \right\} \quad (8)$$

where $\operatorname{Re}\{ \}$ indicates the real part.

The observed pressure spectra at the 4m depth stack (measured with sensor p45, Figure 3) for the four case studies are compared in Figure 9 to predictions based on Eq. 7. The time series of u (measured with sensor uv44, Fig. 3) were transformed to the vertical elevation of the pressure sensor with Eq. 6, and the spectrum and bispectrum of the transformed time-series were substituted in Eq. 7 to obtain a prediction of the pressure spectrum. The agreement between observed and predicted pressure spectra is generally excellent in Cases I, II, and IV (Figure 9a, b, d). In Case III, the observed and predicted spectra diverge at high frequencies (Figure 9c), probably because the nonlinear shallow water approximation is inaccurate in this case with less energetic and higher frequency seas (See Chapter III). Also included in Figure 9 are the predictions without the Bernoulli correction term ε_b . The results show that the Bernoulli term is small in the energetic part of the spectrum, but reduces the pressure spectral levels by as much as a factor 3 at high frequencies.

V. SIMILARITY OF VELOCITY SPECTRA AT HIGH-FREQUENCIES

It has been suggested (Thornton, 1977) that wave spectra in the surf zone are saturated at high frequencies. That is, energy transferred from low to high frequencies through nonlinear interactions is dissipated at the same rate it is transferred, across the spectrum. Based on dimensional arguments, (Thornton, 1977) showed that the horizontal velocity spectrum $E_u(f)$ in the surf zone is proportional to f^{-3} . Observations of horizontal velocity spectra in the surf zone on three California beaches show approximately -3 slopes at high frequencies in agreement with similarity arguments (Thornton, 1977).

The similarity of the high-frequency tail of velocity spectra in the surf zone is examined here with measurements obtained at the 2 and 4m stacks (Figure 3). Measured spectra of the uppermost current meter in each stack (uv21, uv41) were corrected to mean sea level using the transfer function (2a) with the mean square shallow water approximation for the wavenumber k given by the shallow water dispersion relation (3). A standard linear regression analysis was applied between the log of the frequency and the log of the corrected spectral levels over the high frequency range 0.3-0.5 Hz. Examples of the velocity spectra with best-fit lines are given in Figure 10 (same example cases as in Figs. 4-7, 9). In contrast to the strong decay of spectral peak levels between 4 and 2m depth, the spectral levels in the high frequency tail are comparable at the two

sites, suggesting a saturation regime. However the best-fit slopes appear quite variable, ranging from -2 to -4 .

The estimated slopes of the frequency tail of velocity spectra at the 2 and 4m depth sites are summarized for all 125 data records in Figure 11. The estimated slopes are shown versus the ratio between the root-mean-square horizontal velocity and the shallow water wave speed

$$\alpha = \left\{ \frac{\int_0^{0.5H_s} (E_u(f;0) + E_v(f;0)) df}{gh} \right\}^{\frac{1}{2}} \quad (9)$$

which is a measure of nonlinearity ($\alpha \approx H_s / 4h$ in the linear approximation) and can be used as a crude indication of breaking conditions. Both the 4 and 2m depth observations show considerable scatter with slopes ranging from -5.5 to -3 in 4m depth and from -4 to -1 in 2m depth. Despite the scatter, the slopes in 4m depth are generally steeper than in 2m depth, and there is a noticeable trend of decreasing slope with increasing α at both sides. Overall, these observations indicate a continued flattening of the high-frequency tail of velocity spectra in the surf zone and no clear similarity regime. Differences between present observations and those reported by Thornton (1977, 1979)

may be related to the different beach characteristics. Whereas Thornton's observations were collected on planar beaches, the present observations were collected on a barred beach where breaking is more intermittent and localized on the crest of the sand bar.

VI. SUMMARY

Wave kinematics in the strongly nonlinear regimes of breaking or nearly breaking waves are examined with measurements collected during the DUCK94 experiment on a sandy barred beach. A vertical stack of bi-directional current meters and a pressure sensor were deployed at 3 locations along a cross-shore transect in depths of 2, 4 and 8m. Velocity and pressure spectra observed for a wide range of wave conditions are compared with linear and nonlinear transfer functions. Slopes of the high-frequency tail of velocity spectra in the surf zone are also examined and compared with previous measurements.

In the linear approximation, waves obey the dispersion relation (1) and are strongly attenuated over the water column at high frequencies. However, nonlinear interactions transfer energy from the spectral peak to high frequency components that do not obey the dispersion relation (1). In shallow water these nonlinearly forced high frequency components are strongly amplified and significantly change the local wave kinematics. The observed vertical attenuation of horizontal velocity spectra at high frequencies in 8 and 4m depth is much weaker than predicted by linear theory (Figures 4-8). These discrepancies are shown to be consistent with nonlinearly forced high-frequency components that have relatively small wavenumbers and thus are less attenuated than linear waves. The observed vertical decay in 4m depth and to a lesser degree in 8m depth are in good agreement with a simple nonlinear model prediction based on the assumption that the high-frequency tail of the spectrum is dominated by nonlinearly forced components that travel with the shallow water wave speed (i.e. the

speed of the spectral peak components). In 2m depth, differences between the linear and nonlinear transfer function are small and both predictions are in reasonable agreement with the observed weak vertical decay. At infragravity frequencies at the shallower sites, observed velocity spectra often show significant vertical decay that is not predicted by either model. Possible causes for these discrepancies are bottom boundary layer effects (i.e. velocities decrease in a shear layer towards the seabed) and contributions of motions other than gravity waves (e.g., shear instabilities of the longshore current). At the peak frequency, comparisons for the linear and nonlinear models are generally within the accuracy of the instruments.

Observed velocity and pressure spectra in 4m depth are in good agreement with the nonlinear transfer function. It is shown here that the nonlinear Bernoulli term $-u^2/2g$ contributes significantly to the observed high frequency pressure fluctuations and in some cases dominates the high frequency part of the pressure spectrum.

The similarity of the high frequency tail of the observed velocity spectra was examined through a linear regression analysis between the logs of the frequency and spectral levels. Earlier studies (Thornton, 1977, 1979) have suggested that horizontal velocity spectra in the surf zone are saturated at high frequencies with an f^{-3} tail. The best-fit slope values show large variations in both 4m depth (-5.5 to -3 slopes) and 2m depth (-4 to -1 slopes), with a general tendency for spectra to continue to flatten at high frequencies as waves propagate through the surf zone. The differences between the present observation and the -3 slopes observed by Thornton may be related to the different beach characteristics. The present observations were collected on a natural

barred beach with strong localized wave breaking on the sand bar crest, whereas Thornton's observations were collected on planar beaches. Further work is needed to investigate the similarity and saturation of wave spectra in the surf zone.

APPENDIX

FIGURE 1. (a) Example total horizontal velocity spectrum observed in 4m depth (current meter uv41, Figure 3) on September 5 (Case II, discussed in detail below) with distinct harmonic peaks. (b) According to second-order theory the nonlinearly forced harmonic waves are phase-locked to the spectral peak (f_p) components. Hence the harmonic components ($2f_p, 3f_p, 4f_p, 5f_p$) are expected to obey the shallow water dispersion relation (dash-dotted line) rather than the linear finite depth dispersion relation (solid line).

FIGURE 2. Definition sketch for measurements collected at a vertical elevation z . h is the total water depth, and $d (=z+h)$ is the height of the instruments above the sea bed.

FIGURE 3. Vertical stacks of instruments deployed in 2, 4, and 8m depth during the DUCK94 experiment. Squares indicate bidirectional current meters. Triangles indicate pressure sensors.

FIGURE 4. Vertical attenuation of velocity spectra observed in Case I (4 September, 1100-1200 EST). (a-c) The total horizontal velocity spectrum $E_u(f) + E_v(f)$ observed at different vertical elevations in the 2, 4, and 8m stacks. (d-f) Ratio between the predicted and observed attenuation of velocity spectral levels between the uppermost and

lowermost current meters of each stack. Both a linear finite depth model prediction (solid curves, based on Eqs. 1, 2a) and a nonlinear shallow water model prediction (dash-dot curves, based on Eqs 2a, 3) are compared to observations.

FIGURE 5. Vertical attenuation of velocity spectra observed in Case II (5 September, 1200-1300 EST) (same format as Figure 4).

FIGURE 6. Vertical attenuation of velocity spectra observed in Case III (19 September, 12:00-1300 EST) (same format as Figure 4).

FIGURE 7. Vertical attenuation of velocity spectra observed in Case IV (15 October, 2200-2300 EST) (same format as Figure 4). No data was available for the 8m stack.

FIGURE 8. The ratio of predicted to observed attenuation of the velocity variance between the uppermost and lowermost current meters in the high frequency range of 0.3-0.5 Hz based on linear (Eqs. 1, 2a, lower panels) and nonlinear (Eqs. 2a, 3, upper panels) models versus the total velocity variance (over the range 0-0.5 Hz) measured by the uppermost current meter. Results for the 2 and 4m stacks are shown in the left and right panels, respectively. Each asterisk represents a one-hour data record.

FIGURE 9. Comparisons of observed pressure spectra at the 4m stack (solid curves) with predicted spectra based on velocity measurements and the non-linear transfer function (7)

between velocity and pressure spectra (dot-dash-dot curves). Also included are predictions that neglect the Bernoulli term (8) (dotted curve). Results are shown for the same four case studies as in Figures 4-7.

FIGURE 10. Observed total horizontal velocity spectra (corrected to mean sea level) in 4 and 2m for the same four case studies shown in Figs. 4-7. The best-fit lines to the high-frequency (0.3-0.5 Hz) tail of the spectra are indicated with heavy solid lines. The computed high-frequency slopes in 4m depth are (a) -3.5 , (b) -4.1 , (c) -3.8 , (d) -3.7 . In 2m depth the slopes are: (a) -2.0 , (b) -2.1 , (c) -2.8 , (d) -3.1 .

FIGURE 11. Estimated slopes of the velocity spectra (in the 0.3-0.5 range) versus the normalized rms horizontal velocity α for all 125 data records. Results in 4 and 2m depth are indicated with asterisks and squares, respectively.

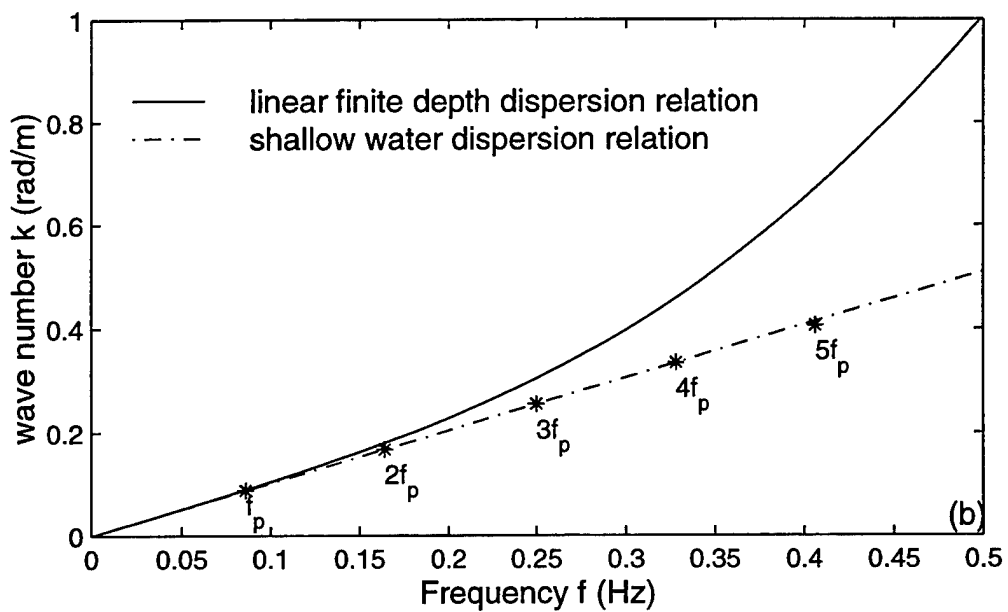
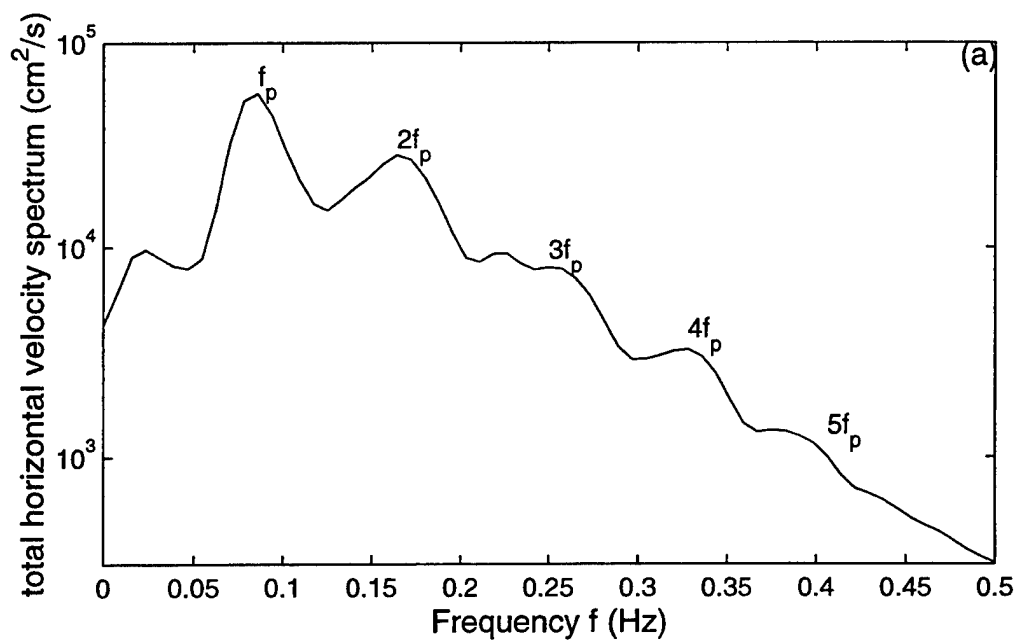


Figure 1

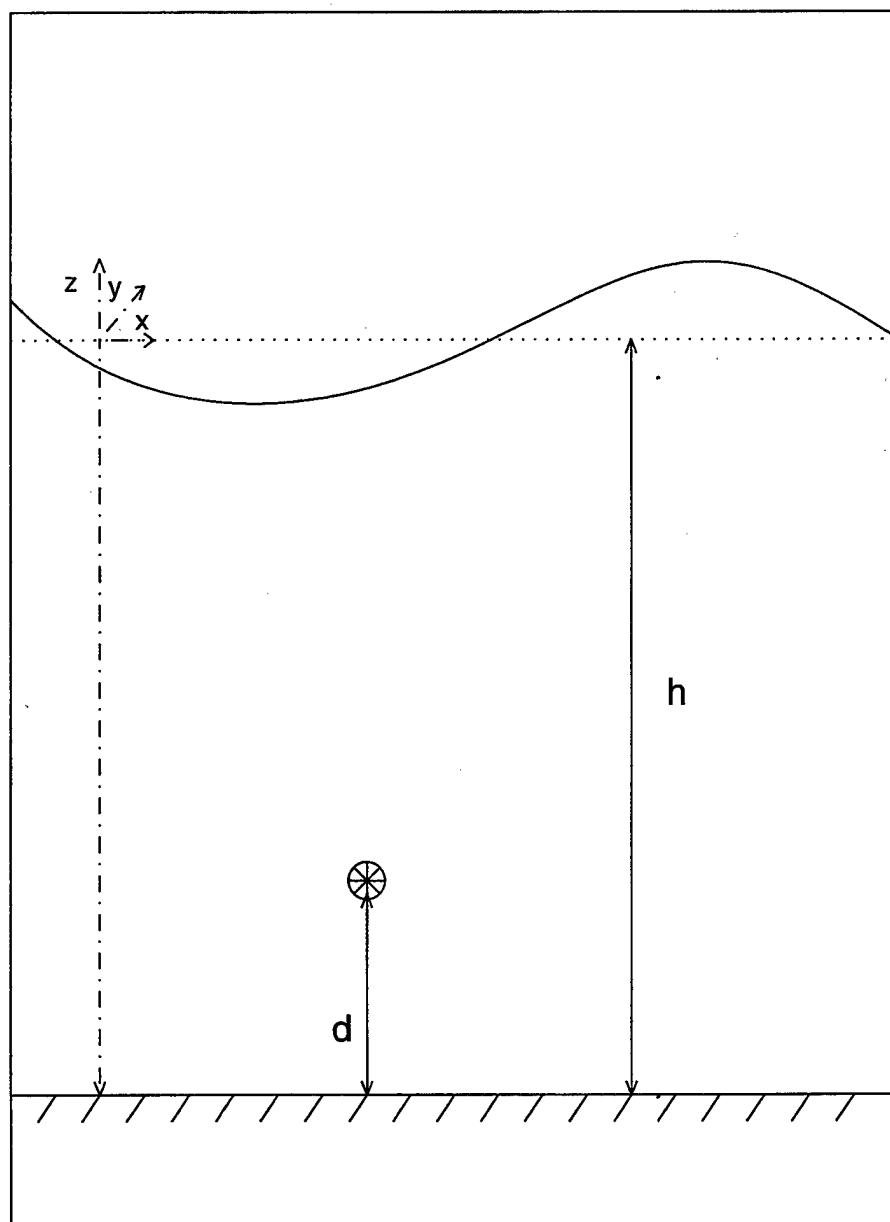


Figure 2

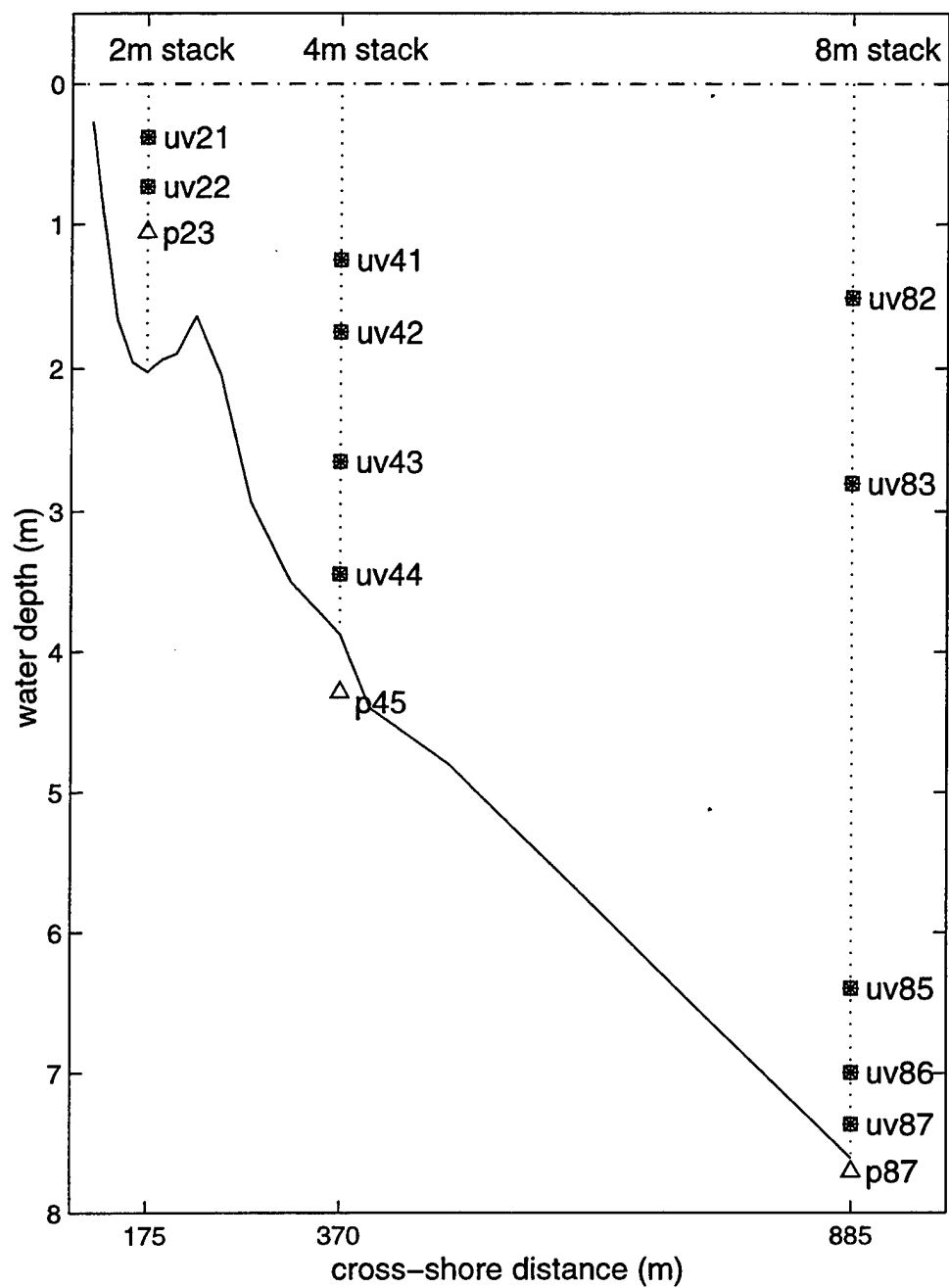


Figure 3

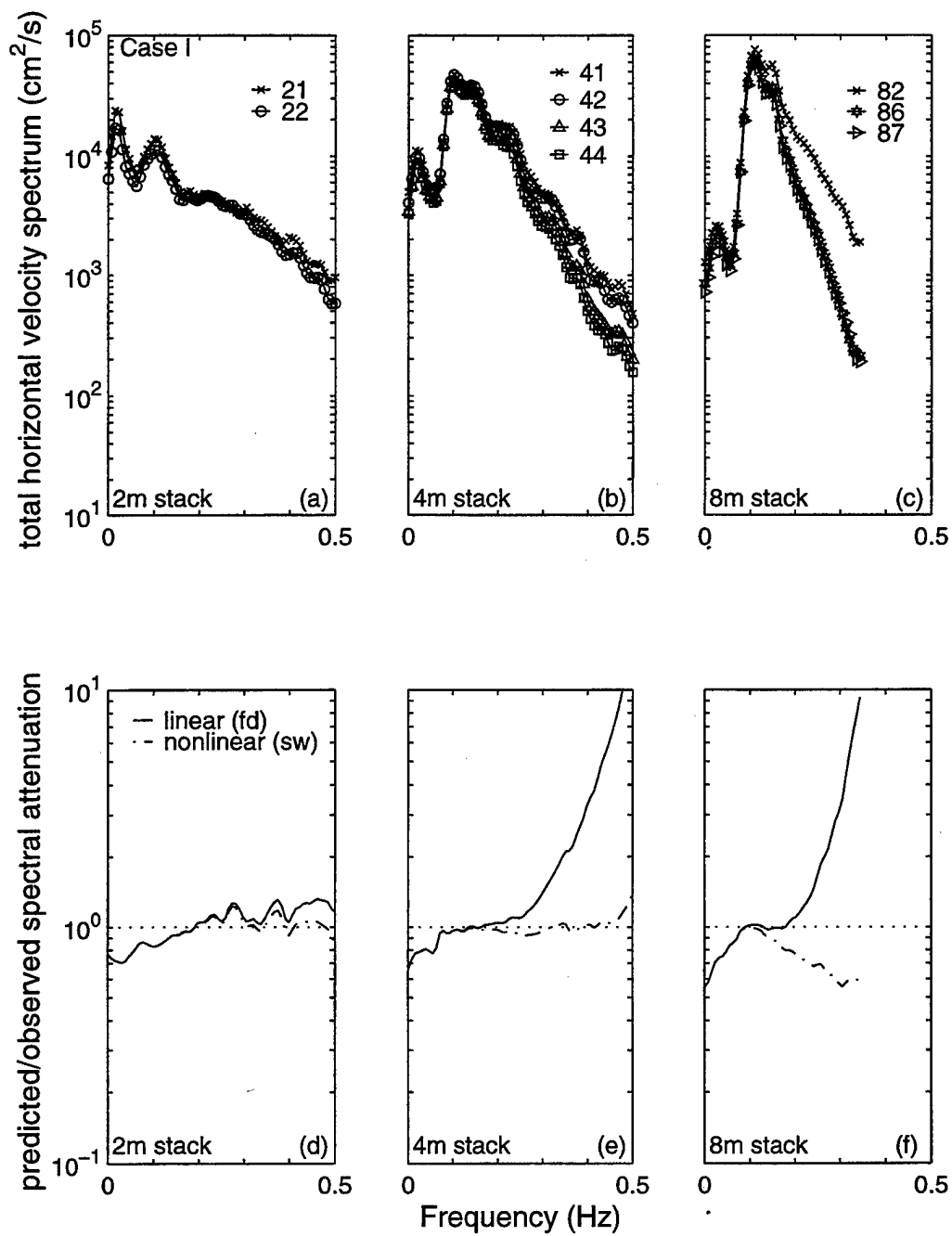


Figure 4

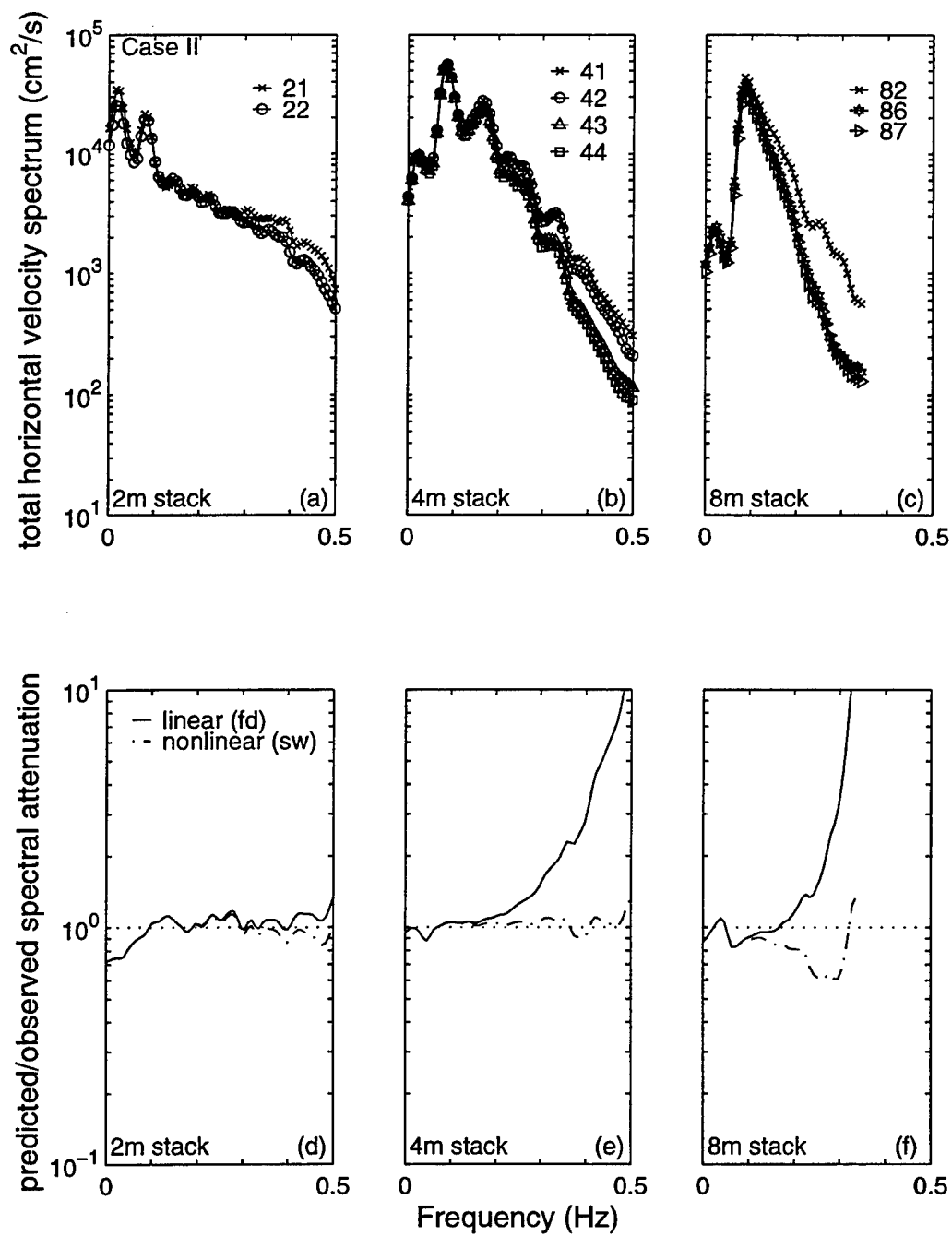


Figure 5

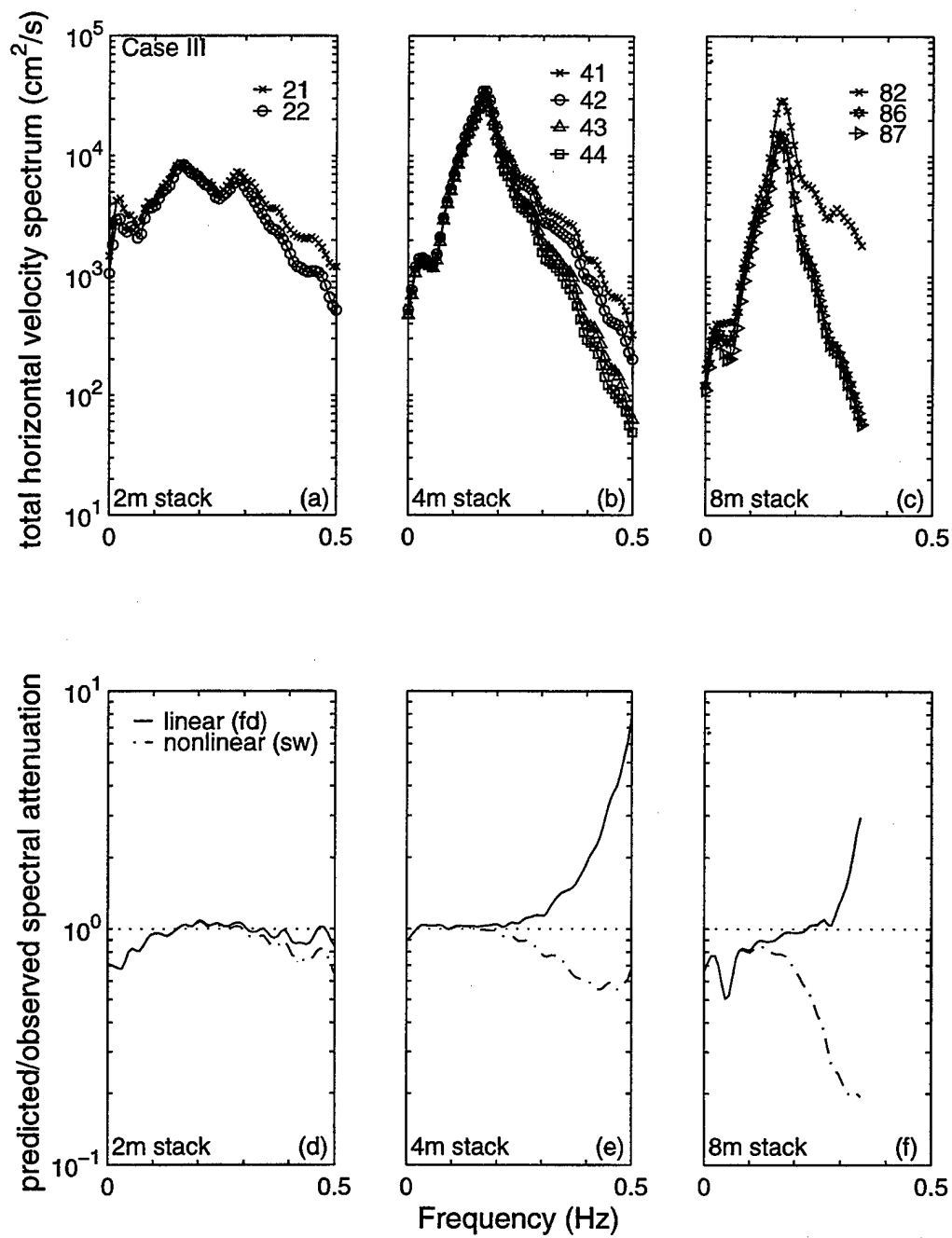


Figure 6

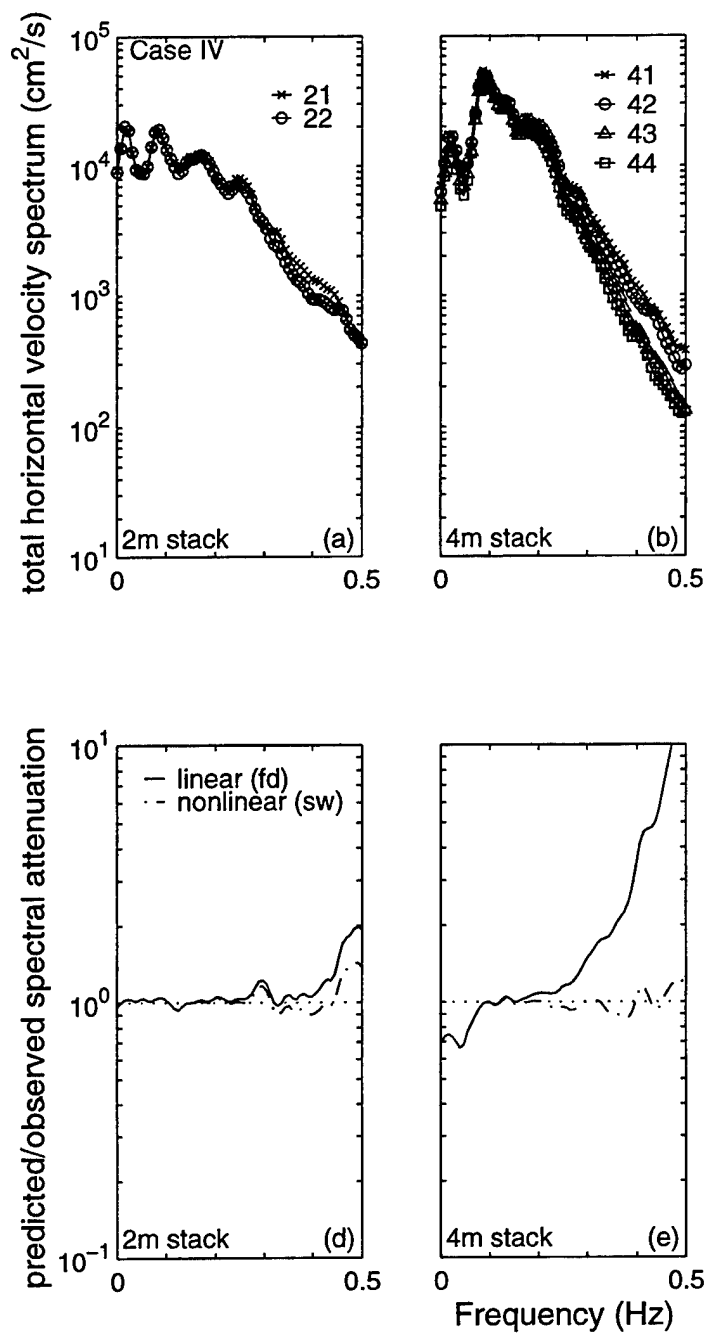


Figure 7

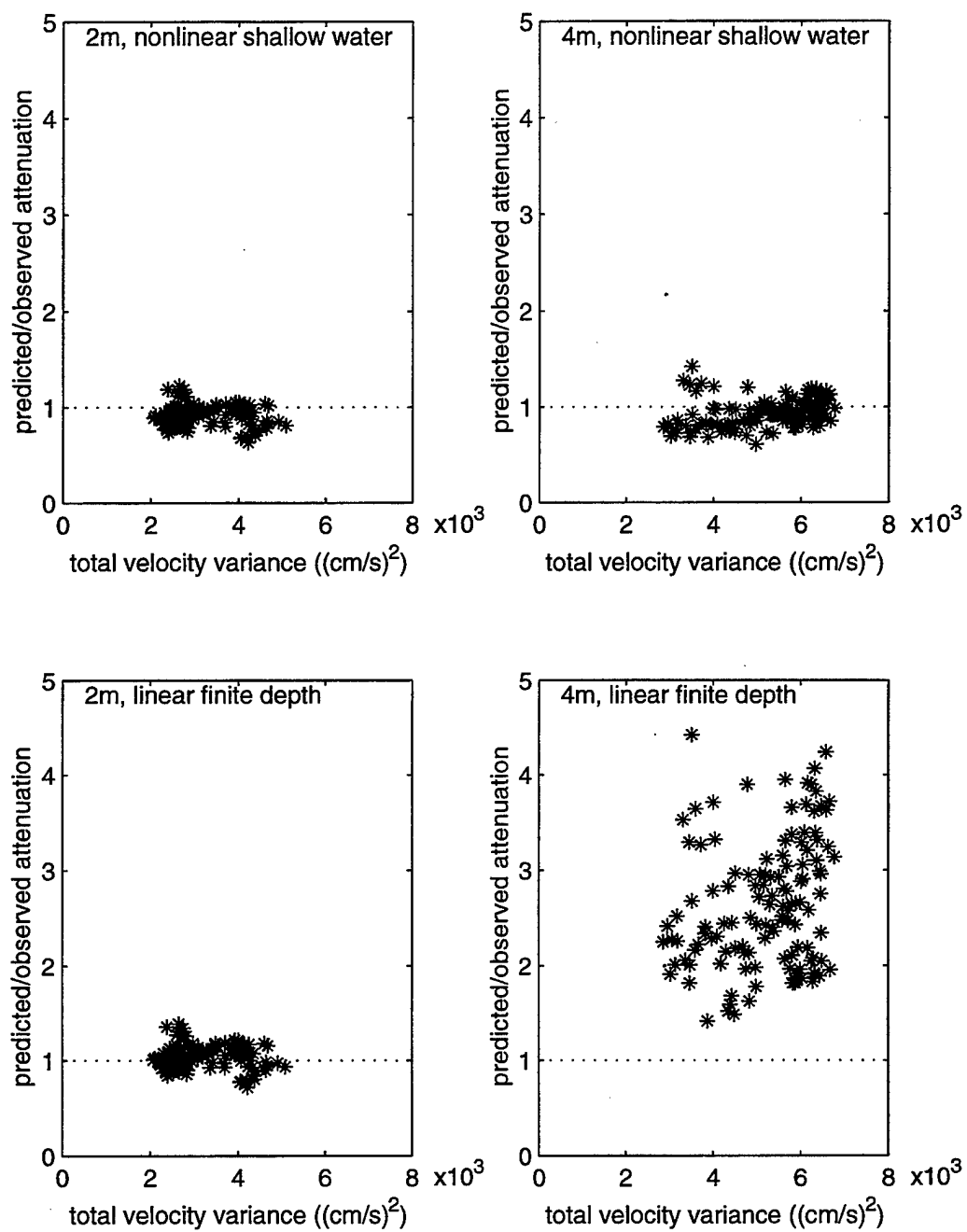


Figure 8

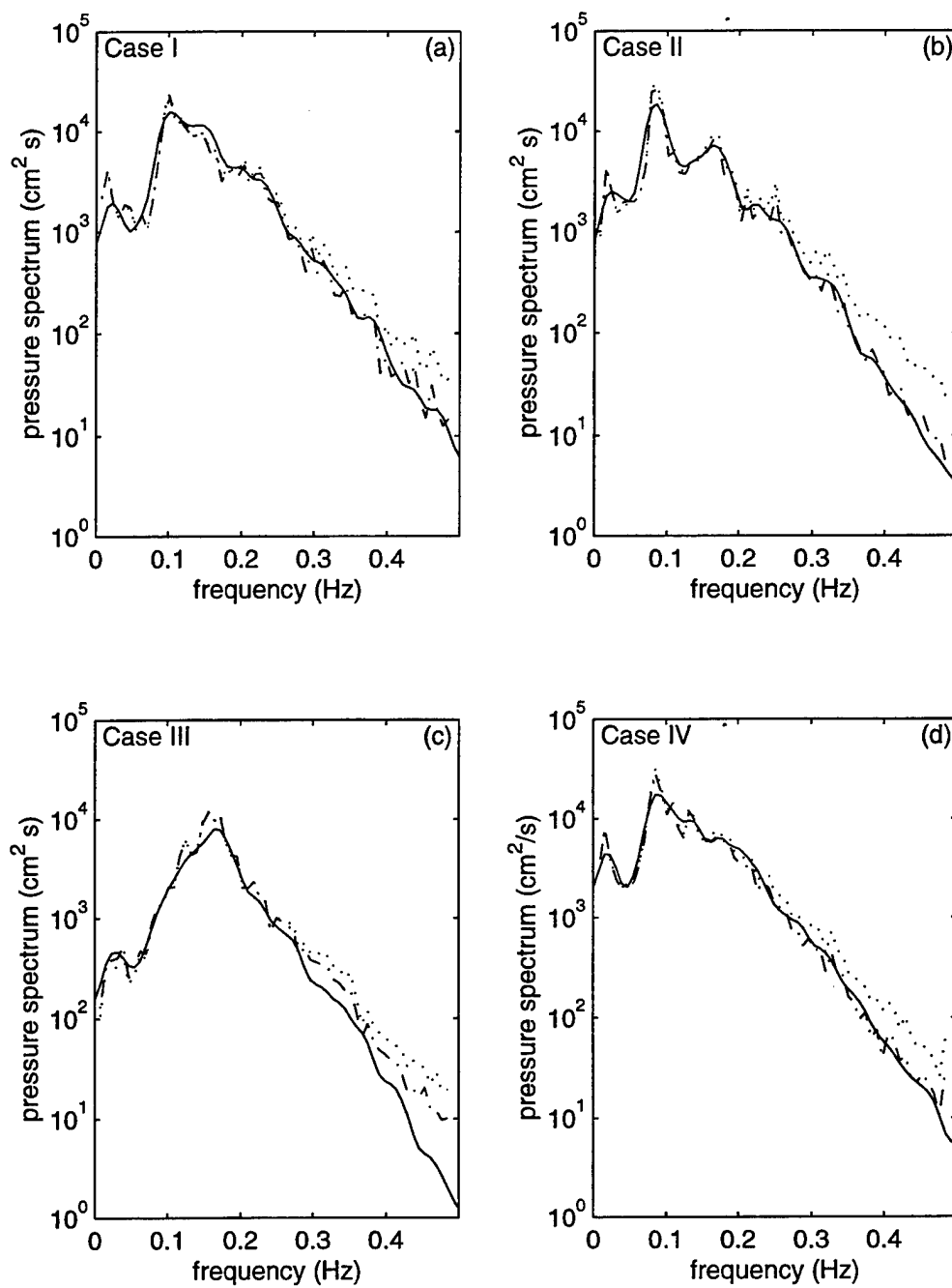


Figure 9

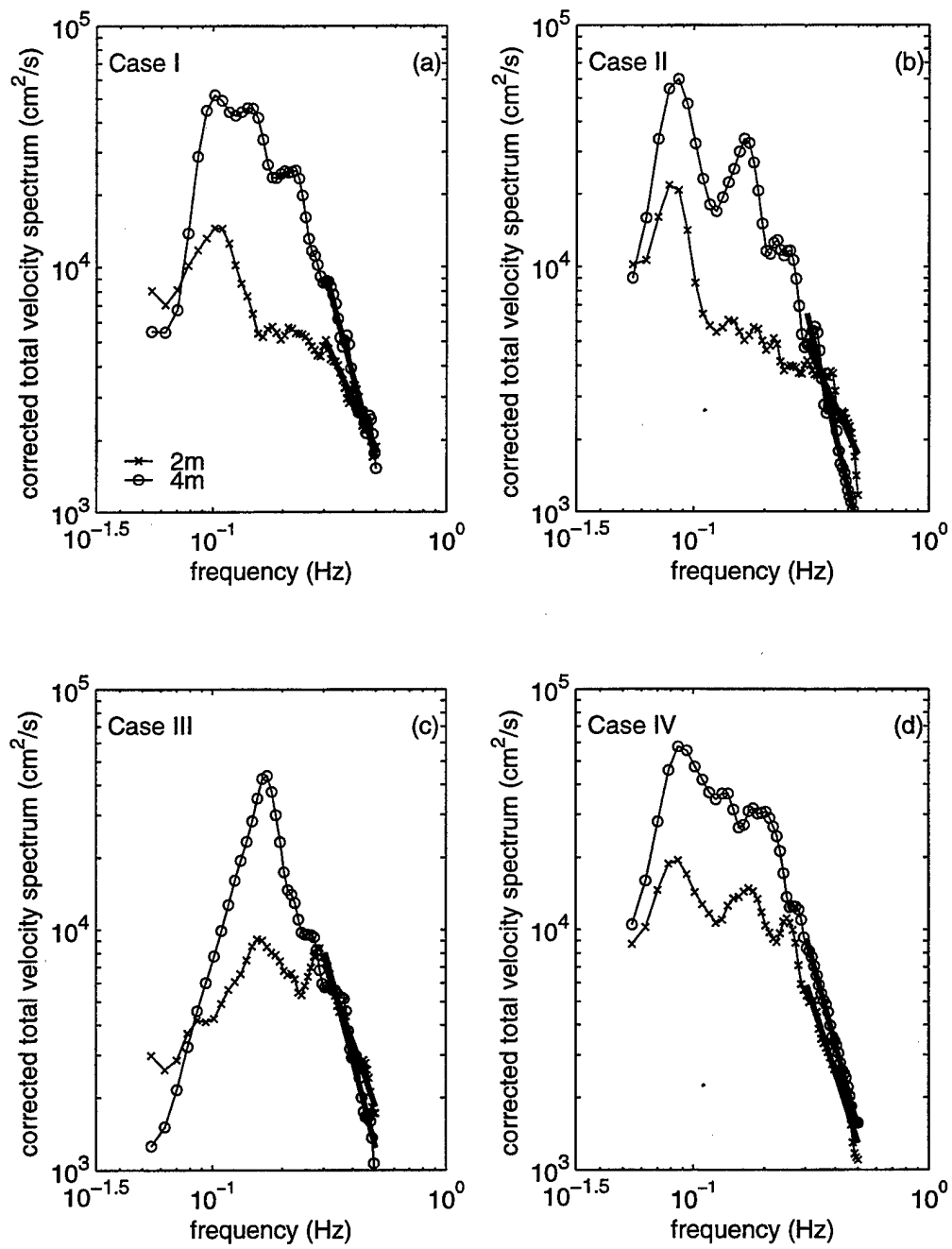


Figure 10

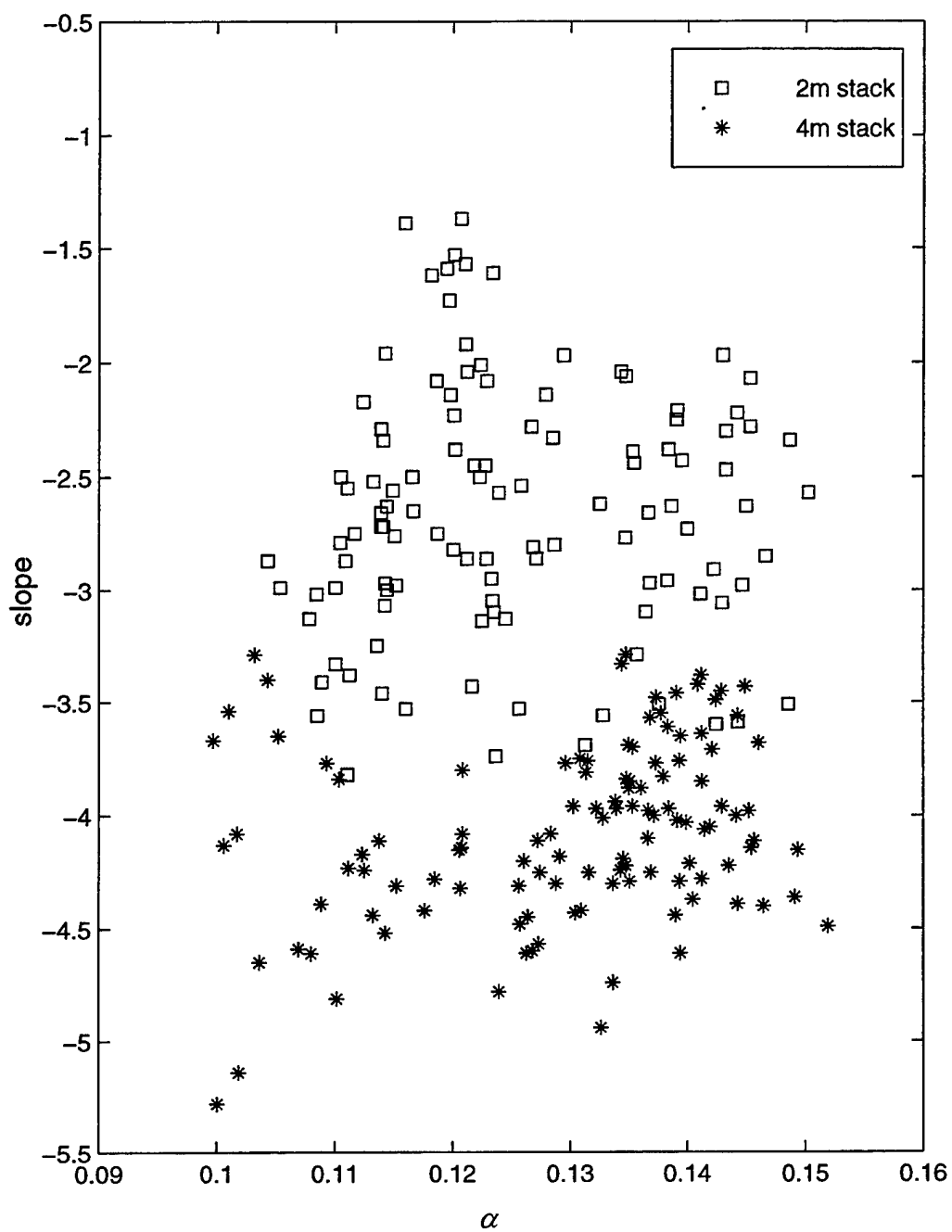


Figure 11

LIST OF REFERENCES

- Donelan, M. A., J. Hamilton, and W. H. Hui, 1985: Directional spectra of wind-generated waves. *Phil. Trans. R. Soc. Lond.*, A315, 509-562.
- Elgar, S., R. T. Guza, B. Raubenheimer, T. H. C. Herbers, and E. L. Gallagher, 1997: Spectral evolution of shoaling and breaking waves on a barred beach. *J. Geophys. Res.*, 102(C7) 15797-15805.
- Herbers, T. H. C., and R. T. Guza, 1991: Wind-wave nonlinearity observed at the sea floor. Part I: Forced-wave energy. *J. Phys. Oceanogr.*, 22, 1740-1760.
- Herbers, T. H. C., and R. T. Guza, 1992: Wind-wave nonlinearity observed at the sea floor. Part II: wavenumbers and third-order statistics. *J. Phys. Oceanogr.*, 22, 489-504.
- Herbers, T. H. C., R. L. Lowe, and R. T. Guza, 1992: Field observations of orbital velocities and pressure in weakly nonlinear surface gravity waves. *J. Fluid. Mech.*, 245, 413-435.
- Herbers, T. H. C., and R. T. Guza, 1994: Nonlinear wave interactions and high-frequency seafloor pressure. *J. Geophys. Res.*, 99, 10035-10048.
- Herbers, T. H. C., S. Elgar, and R. T. Guza, 1994: Infragravity-frequency (0.005-0.05 Hz) motions on the shelf, Part 1: Forced waves. *J. Phys. Oceanogr.*, 24, 917-927.
- Herbers, T. H. C., N. R. Russnogle, and S. Elgar, 1999: Spectral energy balance of breaking waves within the surf zone. Submitted to *J. Phys. Oceanogr.*
- Freilich, M. H., and R. T. Guza, 1984: Nonlinear effects on shoaling surface gravity waves. *Phil. Trans. R. Soc. Lond.*, A311, 1-41.
- Gallagher, E. L., S. Elgar, and R. T. Guza, 1998: Observations of sand bar evolution on a natural beach. *J. Geophys. Res.*, 103, 3203-3215.
- Guza, R. T., and E. B. Thornton, 1980: Local and shoaled comparisons of sea surface elevations, pressures and velocities, *J. Geophys. Res.*, 85, 1524-1530.
- Guza, R. T., M. C. Clifton, and F. Rezvani, 1988: Field intercomparisons of electromagnetic current meters, *J. Geophys. Res.*, 93, 9302-9314.
- Lentz, S., R. T. Guza, S. Elgar, F. Feddersen, and T. H. C. Herbers, 1999: Momentum balances on the North Carolina inner shelf. *J. Geophys. Res.*, in press.

Thornton, E. B., and R. F. Krapohl, 1974: Water particle velocities measured under ocean waves. *J. Geophys. Res.*, 79, 847-852.

Thornton, E. B., 1977: Rederivation of the saturation range in the frequency spectrum of wind-generated gravity waves. *Res.*, 84, 4931-4938.

Thornton, E. B., 1979: Energetics of breaking waves within the surf zone. *J. Geophys. Res.*, 84, 4931-4938.

INITIAL DISTRIBUTION LIST

	No. Copies
1. Defense Technical Information Center 8725 John J. Kingman Rd. STE 0944 Ft. Belvoir, VA 22060-6218	2
2. Dudley Knox Library Naval Postgraduate School 411 Dyer Rd. Monterey, CA 93943-5102	2
3. Professor T.H.C. Herbers, Code OC/He Department of Oceanography Naval Postgraduate School Monterey, CA 93943-5121	6
4. Professor E.B. Thornton, Code OC/Tm Department of Oceanography Naval Postgraduate School Monterey, CA 93943-5121	1
5. P.F. Jessen, Code OC/Js Department of Oceanography Naval Postgraduate School Monterey, CA 93943-5121	1
6. LT Richard K. (Chip) Constantian Jr. P.O. Box 677 Wadesboro, NC 28170	3